IJIE

INTERNATIONAL JOURNAL OF INTEGRATED ENGINEERING
ISSN: 2229-838X e-ISSN: 2600-7916

Vol. 18 No. 3 (2026) 166-176
https://publisher.uthm.edu.my/ojs/index.php/ijie

Analysis of Variance and Surface Response Temperature Interaction on Adsorption Behaviour of Copper in Alkaline Medium

Augustine E. Ubogu[1], Ojo S. I. Fayomi[1, 2], Joshua O. Atiba[1]*

[1] *Department of Mechanical Engineering,*
Bells University of Technology, P.M.B. 1015, Ota, Ogun State, NIGERIA
[2] *Department of Mechanical Engineering Science,*
University of Johannesburg, Auckland Park, Kingsway Campus, P. O. Box 534, Johannesburg, SOUTH AFRICA

*Corresponding Author: atibajoshua7@gmail.com
DOI: https://doi.org/10.30880/ijie.2026.18.03.011

Article Info

Received: 1 July 2025
Accepted: 12 October 2025
Available online: 13 May 2026

Keywords

Copper, fishbone ash, corrosion, Inhibitor, adsorption

Abstract

Copper's susceptibility to chloride-induced deterioration has increased research interest in sustainable corrosion inhibitors. Using electrochemical techniques (potentiodynamic polarisation, open-circuit potential) at temperatures (30–60°C) and concentrations (0.2–0.8 g), this study investigates fishbone ash as a green inhibitor for copper in 0.5 M NaCl. At 30° C/0.8g, the results show mixed-type inhibition behaviour with an efficiency of 98.6% (corrosion rate reduction: 195.96 to 2.69 µm/yr). Temkin adsorption study showed physisorption dominance (ΔG°ads = -10.47 to -12.23 kJ/mol) and high surface interaction (Kads = 1.1475–1.4931 mol^{-1}). optimum performance was found at 53.37°C with 0.49g inhibitor through statistical optimisation using response surface methods, resulting in a predicted corrosion rate of 1.59 µm/yr (99.3% reduction compared to control). With optimal conditions allowing for >98% corrosion suppression, these results confirm fishbone ash's efficacy as an environmentally beneficial inhibitor.

1. Introduction

The favourable properties of copper and its alloys, such as their strong resistance to corrosion, excellent electrical and thermal conductivity, and outstanding mechanical workability and malleability, are highly desired [1, 2]. These qualities are widely applied throughout industries. Copper and its alloys have a wide range of applications, including the production of wires, sheets, and pipelines for the nautical and electronic industries, power plants, heat exchangers, and cooling towers [3, 4]. Even while copper possesses anti-corrosive properties, it can nevertheless deteriorate in some severe environments. The presence of salt ions and other airborne contaminants can dramatically speed up the rate of corrosion of copper, causing corrosion byproducts to build up on the surface [5, 6]. Since copper has so many benefits various industries, it needs to be protected. The use of organic inhibitors stands out among the vital techniques for protecting copper against corrosion. These organic substances predominantly interact with the copper surface to exhibit their inhibitory effects, which is made possible by adsorption [7]. Polar functional groups stabilise the adsorption mechanism by acting as the centre of gravity for the reaction. essentially, the adsorption process, the inhibitor's chemical composition, the kind of electrolyte solution, and the intrinsic characteristics of the metal all influence how an inhibitor adheres to a metal surface [8].

Developing area in corrosion research, organic green inhibitors have characteristics similar to those of traditional inhibitors [9]. These inhibitors, which function through mechanisms such the formation of adsorption coatings, the production of corrosion products that act as passivators, and the production of precipitates that neutralise hazardous components, are essential for both industrial and conservation applications [10]. The creation of a barrier coating that protects against water and corrosive chemicals results from this protective action's physical or chemical adsorption on the metal surface. Organic substances that are rich in polar functional groups and frequently contain heteroatoms improve the effectiveness of organic green corrosion inhibitors by protecting the metal surface from aqueous corrosive species [11]. In certain circumstances, the natural biopolymer chitosan, which is derived from the exoskeletons of crustaceans, has shown extraordinary ability to complex with metallic ions and prevent corrosion [12]. Recently, scientists have focused on the potential of animal bone particles in the prevention of corrosion. [13–16] copper. By examining copper's corrosive behaviour and crucial adsorption properties in an alkaline environment when exposed to fish bone ash, this work seeks to close this gap.

2. Experimental Procedures

2.1 Sample Preparation

Twenty identical samples of the copper plates were cut measuring 10 x 20 x 2 mm each. Then grinding and polishing was done on these samples using different emery paper grits from 80 to 1200 µm. After that they were embedded into epoxy resin, cleaned thoroughly by ultrasonic treatment, and dried in air. Fresh fish bones underwent a thorough cleansing procedure involving acetone and warm water. After this cleansing, the bones were allowed to air-dry for a duration of 98 hours. Subsequently, mechanical crushing was employed to reduce the bone fragments into a fine powder. The obtained bone powder was then sieved to attain a particle size of 600 µm. A batch of 500g of fish bone powder was subjected to calcination at 200°C for a duration of 2 hours. Post-calcination, fish bones were meticulously ground into finer particles. To achieve precise sizing within the range of 100 µm to 45 µm, the fish bone material underwent further refinement, employing carefully selected mechanical sieves.

2.2 Electrochemical/Adsorption Response

Before proceeding to the electrochemical experiments using the copper samples, the samples were firm polish with different grades of emery papers and cleaned afterward with acetone. In the experimental procedure, a three-electrode cell set up was used in which there was a copper working electrode which had an area of exposure equal to 1 cm^2 and a reference electrode made of silver/silver chloride (Ag/AgCl), with a graphite rod as the counter electrode. This was done in order to investigate the behavior of copper corrosion especially in alkaline media containing 3 wt% NaCl active ingredients. The tests were carried out on a Potentiostat Corrtest Portable CS100 at temperatures between 30 and 60 degrees Celsius. Within this time frame, different quantities of the inhibitors were applied stepwise namely 0.2g, 0.4g, 0.6g and 0.8g. It was determined by a scanning rate of 0.001V/sec for the assessment of the anodic and cathodic linear regions. Tafel analysis evaluated the following important parameters of corrosion and adsorption: corrosion rate; current density; linear polarization resistance; corrosion potentials. The inhibition efficiency (%IE) was determined using linear polarization resistance (LPR) which is used together with potentiodynamic corrosion rate and current density to give an overall assessment of copper's corrosion behavior and its inhibition. Based on preliminary trials, inhibitor doses of 0.2–1.0 g L^{-1} were chosen to maximize inhibition without solubility or agglomeration issues; test temperatures of 30 °C (ambient marine conditions) and 60 °C (accelerated conditions) with 3.5 wt % NaCl. Blank runs (no inhibitor) were done on identically polished, ethanol-cleaned coupons following a 120s OCP stabilisation. All tests were conducted in triplicate (≤5% SD) to assure reproducibility and isolate the inhibitor's effect.

2.3 Morphological Study

The surface morphology of the copper samples after undergoing corrosion was examined using a Joel JSM6510 scanning electron microscope equipped with EDS.

2.4 Statistical Analysis and Optimization

The analysis of data from the experiment is focused on understanding the effect or interaction of the exogenous variables rather concentration of inhibitors and working temperature on the property parameter corrosion response. This analysis was conducted using the software Design Expert at a very high confidence level of 95%. Each response has been formulated based on second order regression thus more knowledge is available about these interactions which then facilitate the extension of the use of inhibitors in the future.

Int. Journal of Integrated Engineering Vol. 18 No. 3 (2026) p. 166-176

3. Result and Discussion

3.1 Open Circuit Potential Behaviour of Copper

The Open Circuit Potential (OCP) profiles of copper in a NaCl environment and inhibited by fishbone ash are shown in Figures 1 and 2. These measurements were made before the experiment began and after it had finished. The experiment was carried out at two distinct temperatures, 30°C and 60°C, respectively. Figure 1 shows a clear decrease shift in potential over a 120-second period after the addition of fishbone as an inhibitory agent. This change indicates that reactions occur at the cathode more frequently than at the anode. Both the uninhibited samples and the least inhibited samples had potentials between -0.1 and -0.3V as the graph's potential values stabilised [17]. Focusing on Figure 2, the plot trends showed that as concentration of fishbone increased for the inhibited samples, the region shifted towards the positive. Additionally, the effect of high temperatures on the metal surface backed anodic reactions rather than cathodic reactions [18–21].

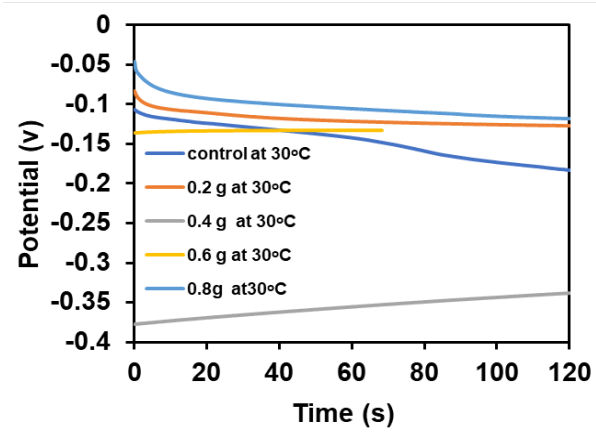

Fig. 1 *Open circuit potential plot for fishbone ash Inhibition at 30°C*

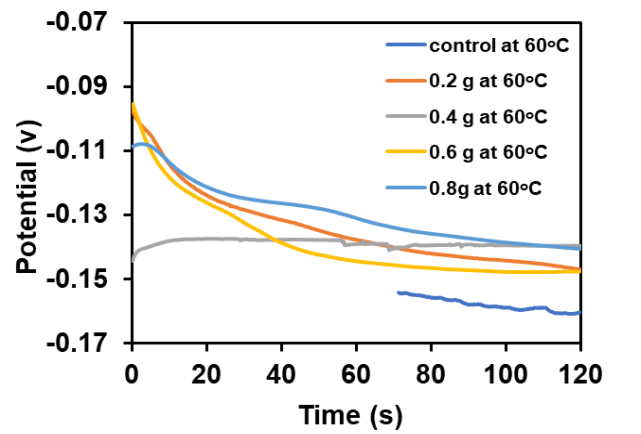

Fig. 2 *Open circuit potential plot for fishbone ash Inhibition at 60°C*

3.2 Potentio-Dynamic Polarization Analysis of Copper

As summarized in Table 1, the effect of different concentrations of fishbone inhibitors on the copper corrosion in NaCl environment is studied in terms of its electrochemical behaviour. Relevant parameters include the corrosion rate (mm/year), polarisation resistance (PR) (Ω), current density (J_{CORR}) (A/cm^2) and corrosion potential (E_{CORR}) (V). It is apparent that increase in fishbone inhibitor concentration leads to decreased corrosion rate. A rise in inhibitor concentration induced a very remarkable corrosion rate (CR) drop of about 98.6% (193.27 µm/yr) at 30 °C on copper surface while similarly significant decreases were noted at CR averaged 177.30 µm/yr at 40 °C. This trend was still present at 50 °C and 60°C where CR decreased by 99.29% and 90.21%, respectively. Importantly, irrespective of sample sets and temperature variations displayed, there always appeared to be a tendency for E_{CORR} data presented in Table 1 and Figures 3 and 4 to move towards more positive (anodic) values. Furthermore,

the E_{CORR} variation stayed less than 0.085V under all temperature conditions. This indicates mixed-type inhibitory behaviour on the part of fishbone inhibitor [22–25].
The process of corrosion at both the cathode and anode regions of copper within an environment of NaCl and fish can be explained as follows:

Anodic reactions:

$$Cu - e^- \rightarrow Cu^+_{ads} \quad (1)$$

$$Cu^+_{ads} - e^- \rightarrow Cu^{2+}_{sol} \quad (2)$$

Cathodic reaction:

$$O_2 + 2H_2O + 4e^- \rightarrow 4OH^- \quad (3)$$

It is now rather straightforward to explain the copper adsorption and solubility behaviour of Cu^+_{ads} and Cu^{2+}_{sol}species in Chloride containing solution from the foregoing equations 1 and 2 [26]. According to the equation of the cathodic reaction provided in equation 3, the pH of the sodium chloride solution will post the electrochemical testing, rise marginally because of OH- ions which will be liberated [27].

Mechanism of Adsorption on copper surface:
The copper surface is enhanced by an adsorbed layer of fish bone ash that forms a Cu+ compound thus preventing the metal from Cl- ions. This is described in equation 4 below [18, 28]. Generally, there are various factors governing the process of adsorption including but not limited to the inhibitor's chemical structure, character of the metal surface, relationship between organic compounds and its surfaces as well as corrosive electrolyte composition [29].

$$Cu^+_{ads} + nCBA \rightarrow [Cu - FBA_n]^+_{ads} \quad (4)$$

Table 1 *Tafel data of copper inhibited samples*

Temp. (°C)	Conc. (g)	E_{CORR} (V)	J_{CORR} (A/cm²)	CR (μm/yr)	PR (Ω)
30	Control	-0.304294	1.69E-05	195.963	54.513
	0.2	-1.26729	4.33E-04	53.7861	5.629
	0.4	-1.29486	3.66E-04	42.5004	7.1243
	0.6	-0.513407	5.85E-04	6.80047	44.525
	0.8	-0.374798	2.31E-04	2.6893	44.576
40	Control	-1.33383	1.54E-05	179.316	168.858
	0.2	-0.962545	-3.88E-04	45.1139	6.7116
	0.4	-0.593989	-2.11E-04	24.487	12.365
	0.6	-0.465498	8.97E-04	10.4195	29.059
	0.8	-0.39329	1.73E-04	2.01573	50.213
50	Control	-0.936825	1.88E-05	218.959	38.285
	0.2	-1.17191	1.08E-04	45.1840	7.418
	0.4	-0.593989	-2.45E-04	21.8465	0.374
	0.6	-0.401559	2.44E-04	2.83463	10.818
	0.8	-0.350539	1.35E-04	1.56334	19.368
60	Control	-0.663104	9.66E-06	112.247	69.751
	0.2	-1.1228	1.81E-04	40.5250	7.235
	0.4	-0.747266	2.40E-04	27.9056	10.850
	0.6	-0.509157	6.65E-04	7.73159	39.163
	0.8	-0.32675	4.72E-04	5.49008	55.152

Int. Journal of Integrated Engineering Vol. 18 No. 3 (2026) p. 166-176

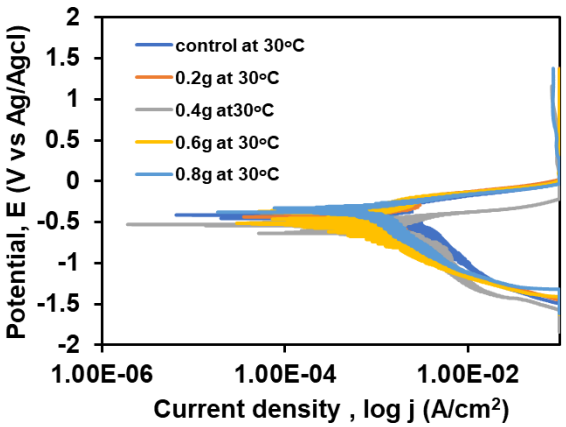

Fig. 3 *Polarization plot for fish bone inhibition @ 30°C*

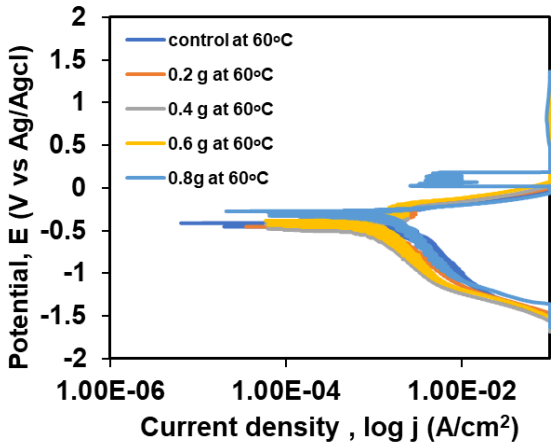

Fig. 4 *Polarization plot for fish bone inhibition at 60°C*

3.3 Fishbone Ash Adsorption Isotherms

To understand the interaction mechanisms of the inhibitor and the surface of the metal, the utilization of adsorption isotherms most play a key role. There are several mathematical models by which this is analysed namely Temkin, Langmuir, Boris-swinkels and Frumkin just to mention a few. For this study the Temkin isotherm was used to investigate the metal-inhibitor reaction has its model (equation 5) best fit the data the electrochemical and potentiodynamic polarization empirical data. This finding emphasizes the significance of understanding the Temkin adsorption isotherm and the impact of the inhibitor's adsorption on its corrosion inhibitive effect [17], [30].

$$\theta = BK_{ads} + B\ln C_{inh} \quad (5)$$

The value denoted by the constant B is understood as the heat of adsorption. The isotherm explains the interaction of adsorbent and adsorbate. The models extrapolate that the adsorption heat of all the molecules present in the layer will exhibit a linear decline with increase in coverage rather than a logarithmic drop, as is illustrated in Figure 5. Values of the parameters K_{ads} (mol^{-1}), G_{ads}($KJmol^{-1}$) and R^2 for the Temkin adsorption model are illustrated in Table 2 [31–33]. Between adsorbent and adsorbate, there is a force called K_{ads}. Greater adsorption leads to larger K_{ads} values hence greater effectiveness of inhibition. This means that as temperature increases from 30 to 60°C the values of K_{ads} increase (1.1475 - 1.4931 mol^{-1}) indicating that fishbone ash adsorbs on copper surface very effectively Table 2. $G°_{ads}$ explains how stable the coating remains on copper surface and its mechanism is uncertain because it varies randomly depending on time. However, these $G°_{ads}$ indicate that higher temperatures make the adsorbed layer more stable since their absolute values are greater than those at lower temperatures. Thus, this may be due to stronger attraction to adsorbent as well as increased mobility of ions and molecules within solution which might make adsorption process more favorable at elevated temperatures than under normal conditions or even below room temperature level respectively. It is worth mentioning that $G°_{ads}$ values greater than or equal to -20 kJ/mol, pertain to physical adsorption, while -40 kJ/mol and above pertains to

chemical adsorption. Adsorption free energy ($G°_{ads}$) values of -10.4663 to -12.2316 kJ/mol, strongly suggest that adsorption is primarily through physisorption, a fact confirmed by the calculations provided [34–37].

Table 2 *Temkin isotherm adsorption parameters*

Temp. (°C)	K_{ads}(mol^{-1})	ΔG_{ads} (KJmol^{-1})	R^2	ln(K_{ads})	1/T	ΔG_{ads}/T	B
30	1.1475	-10.4663	0.8577	0.1376	0.0033	-0.0345	190.8007
40	1.1803	-10.8850	0.9990	0.1657	0.0032	-0.0348	174.9427
50	1.6962	-12.2068	0.5944	0.5284	0.0031	-0.0378	400.0587
60	1.4931	-12.2316	0.8502	0.4008	0.0030	-0.0367	1348.7730

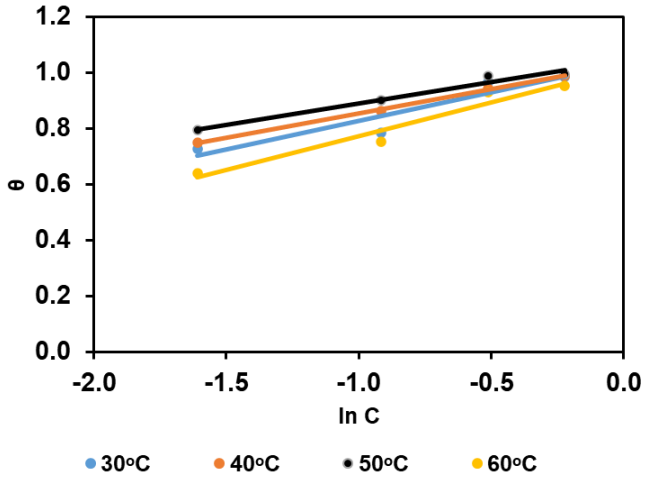

Fig. 5 *A graph of Θ against ln C*

3.4 Microstructural Analysis

Figure 6a–c, which compares untreated copper with fishbone inhibition at concentrations of 0.2g and 0.6g while operating at 60°C, shows SEM pictures of copper samples following corrosion. In Figure 6a, the control sample in the 3 wt% NaCl solution exhibits homogeneous surface disintegration. Figures 6b and 6c, on the other hand, show copper surfaces treated with fishbone inhibition (0.2g and 0.6g concentrations), demonstrating the value of a barrier. The typical stress-induced surface degradation found in untreated samples seems to be prevented by this layer. Figure 6b shows the noodle-like structure that develops when active corrosion sites on the copper surface are filled by adsorption. However, at this lower concentration, some regions are still exposed and vulnerable to Cl- ion attack, which explains why copper has a lesser resistance to corrosion in NaCl. As observed in Figure 6c, larger nodes are seen at greater inhibitor concentrations, leading to a surface that is comparatively smoother and protected by passivated coatings. The physiochemical processes that caused surface recrystallization rather than the anticipated degradation are the cause of this better surface condition.

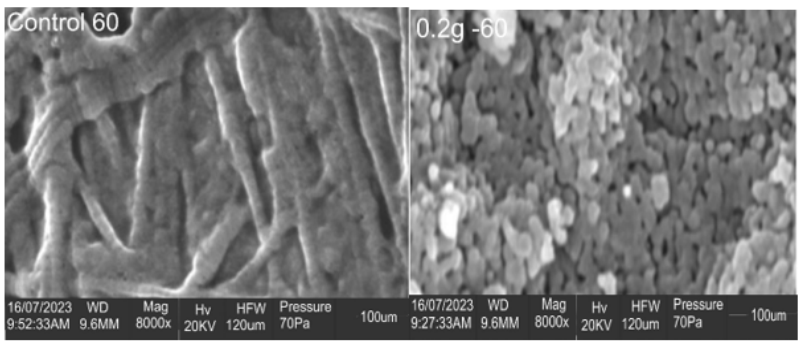

(a) **(b)**

Int. Journal of Integrated Engineering Vol. 18 No. 3 (2026) p. 166-176

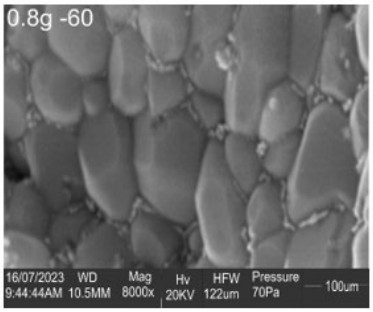

(c)

Fig. 6 *SEM images of copper in NaCl at 60°C (a) Control; (b) 0.2g of fishbone; (c) 0.8g of fishbone*

3.5 Mathematical Optimization of the Corrosion Rate

Table 3 below shown a detail experimental design which identifies the major factors affecting corrosion behaviour of copper samples submerged in a NaCl/fishbone environment. The best combination was found to be 50°C with an inhibitor concentration of 0.8g giving rise to a rate of corrosion equal to 1.56334 mm/year. Table 4 was carefully created by closely examining this experimental framework and utilising the main composite design process. A quadratic equation model that effectively captured the multifaceted interaction of the influencing elements on copper's corrosion rate response (equation 6) took precedence within this table. By an extraordinarily high F-value (23.81) in comparison to an equally remarkably low P-value (0.0001), the prominent features of this model have been highlighted; indicating its outstanding relevance and constant trustworthiness for predicting corrosion rate responses. The model inputs, particularly temperature, inhibitors concentration, and their interactions (A, B, and B^2) in combination, led to a considerable outcome on the corrosion rate. It is also evident from the high R squared values, the relative closeness or R squared values (predicted and adjusted) and consequently low CV% values that the model can predict and replicate the real data accurately [38, 39]. Effective Figure 7 demonstrates how two of these important factors influence the fishbone ash corrosion inhibitor in copper - the second diagram is of key importance. Statistical examining confirmed that the lowest corrosion rate, 1.594 was reached at the temperature of 53.372°C and using a fishbone ash concentration of 0.490 g. A hub of optimal performance in the context of fishbone inhibition for copper corrosion is revealed by this synchronisation of components.

$$R = 20.50 - 8.83A - 77.31B + 14.21AB - 6.31A^2 + 70.76B^2 \quad (6)$$

Table 3 *Empirical design for statistical optimization*

Runs	Temp. (°C)	Conc. (g)	CR (μm/yr)
1	30	0.6	6.80047
2	30	0.4	42.5004
3	50	0	218.959
4	60	0	112.247
5	60	0.2	40.525
6	40	0.2	45.1139
7	40	0.8	2.01573
8	40	0.4	24.487
9	50	0.8	1.56334
10	60	0.6	7.73159
11	60	0.8	5.49008
12	50	0.2	45.184
13	40	0.6	10.4195
14	40	0	179.316
15	30	0.2	53.7861
16	50	0.6	2.83463

Runs	Temp. (°C)	Conc. (g)	CR (µm/yr)
17	30	0.8	2.6893
18	60	0.4	27.9056
19	50	0.4	21.8465
20	30	0	195.963

Table 4 *Analysis of Variance (ANOVA) of fishbone ash inhibition on copper*

Source	SS	DF	MS	F-value	p-value	Remark
Model	79444.85	5	15888.97	23.81	< 0.0001	sig.
A-Temp.	8670.21	1	867.21	13.01	< 0.0001	Sig.
B-Conc.	59774.23	1	59774.23	89.56	< 0.0001	Sig.
AB	1122.58	1	1122.58	1.68	0.2156	Not. sig
A^2	157.37	1	157.37	0.2358	0.6348	Not. sig
B^2	17523.46	1	17523.46	26.26	0.0002	Sig.
Residual	9343.74	14	667.41			
Cor Total	887880.58	19				

R^2 = 89.48%; Adjusted **R^2 =** 85.72%; predicted **R^2 =** 77.71%; CV%= 9.33
**** Sig.- Significant; DF- Degree of Freedom; SS- Sum of square; MS- Mean square****

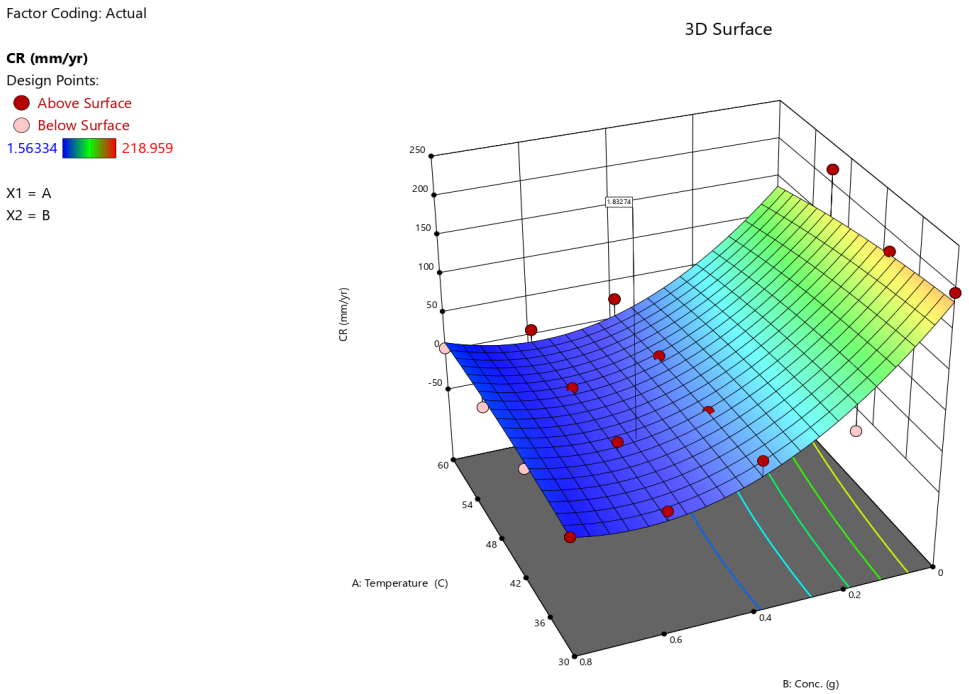

Fig. 7 *Temperature and concentration interplay on the rate of copper corrosion*

4. Conclusion

From the experiments we can made the following conclusions:

- Fishbone ash exhibits mixed-type inhibition behaviour, influencing both cathodic and anodic activities.
- Trends in the Temkin Adsorption parameter (K_{ads}) show a positive response of the metal surface to inhibitor adsorption.
- Gibbs free energy calculations suggest physisorption as the mechanism, indicating physical adsorption rather than chemical.
- Experimental results are confirmed by ANOVA analysis for their consistency and reliability; moreover, optimization analyses show the best experimental conditions which include temperature of 53.372°C and a concentration level of 0.490g.

Although fishbone ash inhibits copper in NaCl on a laboratory scale, it confronts hurdles in industrial applications due to feedstock unpredictability, supply chain scalability, pre-treatment processes, and residue environmental management. Future work will focus on standardising ash quality, optimising processing routes, and ensuring compatibility with current corrosion prevention systems.

Acknowledgement

We greatly value the support that we receive from The Bells University of Technology.

Conflict of Interest

Authors declare that there is no conflict of interest regarding the publication of the paper.

Author Contribution

The authors confirm contribution to the paper as follows: ***study conception and design:*** *Augustine E. Ubogu, Ojo S. I. Fayomi, Joshua O. Atiba.;* ***data collection:*** *Joshua O. Atiba;* ***analysis and interpretation of results:*** *Augustine E. Ubogu, Ojo S. I. Fayomi, Joshua O. Atiba;* ***draft manuscript preparation:*** *Joshua O. Atiba. All authors reviewed the results and approved the final version of the manuscript.*

References

[1] Li, M., & Zinkle, S. J. (2012). Physical and mechanical properties of copper and copper alloys. Elsevier. https://doi.org/10.1016/B978-0-08-056033-5.00122-1

[2] Quartarone, G., Battilana, M., Bonaldo, L., & Tortato, T. (2008). Investigation of the inhibition effect of indole-3-carboxylic acid on the copper corrosion in 0.5 M H_2SO_4. Corrosion Science, 50(12), 3467–3474. https://doi.org/10.1016/j.corsci.2008.09.032

[3] Duran, B., Bereket, G., & Duran, M. (2012). Electrochemical synthesis and characterization of poly(m-phenylenediamine) films on copper for corrosion protection. Progress in Organic Coatings, 73(2–3), 162–168. https://doi.org/10.1016/j.porgcoat.2011.10.008

[4] Duran, B., Bereket, G., Turhan, M. C., & Virtanen, S. (2011). Poly(N-methyl aniline) thin films on copper: Synthesis, characterization and corrosion protection. Thin Solid Films, 519(18), 5868–5874. https://doi.org/10.1016/j.tsf.2011.02.084

[5] Tan, B., et al. (2022). Insight into the anti-corrosion performance of two food flavors as eco-friendly and ultra-high-performance inhibitors for copper in sulfuric acid medium. Journal of Colloid and Interface Science, 609, 838–851. https://doi.org/10.1016/j.jcis.2021.11.085

[6] Tan, B., et al. (2021). Papaya leaves extract as a novel eco-friendly corrosion inhibitor for Cu in H_2SO_4 medium. Journal of Colloid and Interface Science, 582, 918–931. https://doi.org/10.1016/j.jcis.2020.08.093

[7] Fontana, M. G., & Stactile, W. (1970). Corrosion Science and Technology (Vol. 1, p. 149). Plenum Press. https://doi.org/10.1007/978-1-4615-8252-6

[8] Raja, P. B., & Sethuraman, M. G. (2008). Natural products as corrosion inhibitors for metals in corrosive media: A review. Materials Letters, 62(1), 113–116. https://doi.org/10.1016/j.matlet.2007.04.079

[9] Kesavan, D., Gopiraman, M., & Sulochana, N. (2012). Green inhibitors for corrosion of metals: A review. Chemical Science Review and Letters, 1(1), 1–8. https://doi.org/10.5281/zenodo.19496281

[10] Goni, K., & Mazumder, M. A. J. (2019). Green corrosion inhibitors. Corrosion Inhibitors, 30(4), 77–83. https://doi.org/10.5772/intechopen.81376

[11] Popoola, L. T. (2019). Organic green corrosion inhibitors (OGCIs): A critical review. Corrosion Reviews, 37(2), 71–102. https://doi.org/10.1515/corrrev-2018-0058

[12] Jmiai, A., et al. (2017). Chitosan as an eco-friendly inhibitor for copper corrosion in acidic medium: Protocol and characterization. Cellulose, 24, 3843–3867. https://doi.org/10.1007/s10570-017-1381-z

[13] Loto, R. T., & Busari, A. (2019). Electrochemical study of the inhibition effect of cow bone ash on the corrosion resistance of mild steel in artificial concrete pore solution. Cogent Engineering, 6(1), 1644710. https://doi.org/10.1080/23311916.2019.1644710

[14] Zhang, Q., Li, H., Feng, H., & Jiang, T. (2020). Effect of bagasse ash admixture on corrosion behavior of low carbon steel reinforced concrete in marine environment. International Journal of Electrochemical Science, 15(7), 6135–6142. https://doi.org/10.20964/2020.07.65

[15] Loto, R. T., & Busari, A. A. (2022). Inhibition effect of cow bone soot on low carbon steel corrosion in artificial concrete pore environment. Journal of Physics: Conference Series, 2256(1), 012024. https://doi.org/10.1088/1742-6596/2256/1/012024

[16] Omoegun, O. G., Fayomi, O. S. I., & Atiba, J. O. (2023). Investigation of the corrosive behavior and adsorption parameters of copper in a cowbone ash-inhibited alkaline environment. Journal of Bio-Tribo-Corrosion, 9(4). https://doi.org/10.1007/s40735-023-00794-1

[17] Elendu, I. O., Odulanmi, O. A., Fayomi, O. S. I., Williams, A. B., & Daramola, M. (2021). Passivation behaviour and localized corrosion activities of non-toxic surfactant derivatives on copper. IOP Conference Series: Materials Science and Engineering, 1107(1), 012224. https://doi.org/10.1088/1757-899X/1107/1/012224

[18] Tasić, Ž. Z., Petrović Mihajlović, M. B., Radovanović, M. B., & Antonijević, M. M. (2018). Electrochemical investigations of copper corrosion inhibition by azithromycin in 0.9% NaCl. Journal of Molecular Liquids, 265, 687–692. https://doi.org/10.1016/j.molliq.2018.03.116

[19] Sherif, E.-S. M., Erasmus, R. M., & Comins, J. D. (2010). In situ Raman spectroscopy and electrochemical techniques for studying corrosion and corrosion inhibition of iron in sodium chloride solutions. Electrochimica Acta, 55(11), 3657–3663. https://doi.org/10.1016/j.electacta.2010.01.117

[20] Jiménez, Y. S., Gil, M. T., Guerra, M. T., Baltes, L., & Rosca, J. M. (2009). Interpretation of open circuit potential of two titanium alloys for long-time immersion in physiological fluid. Bulletin of the Transilvania University of Braşov, 2, 51. Link

[21] Opadoyin, P. O., Fayomi, O. S. I., & Atiba, J. O. (2024). Investigation of a hydrophobic and sustainable multifaceted coating for enhanced service life of steel. Journal of Bio-Tribo-Corrosion. https://doi.org/10.1007/s40735-024-00913-6

[22] Oguzie, E. E., Li, Y., & Wang, F. H. (2007). Effect of cysteine on the corrosion behaviour of low carbon steel in sulphuric acid. Electrochimica Acta, 53(2), 909–914. https://doi.org/10.1016/j.electacta.2007.07.076

[23] Sherif, E. M., & Park, S.-M. (2006). Effects of 2-amino-5-ethylthio-1,3,4-thiadiazole on copper corrosion as a corrosion inhibitor in aerated acidic pickling solutions. Electrochimica Acta, 51(28), 6556–6562. https://doi.org/10.1016/j.electacta.2006.04.047

[24] da Silva, A. B., Agostinho, S. M. L., Barcia, O. E., Cordeiro, G. G. O., & D'Elia, E. (2006). The effect of cysteine on the corrosion of 304L stainless steel in sulphuric acid. Corrosion Science, 48(11), 3668–3674. https://doi.org/10.1016/j.corsci.2006.02.003

[25] Rehim, S. S. A., Hazzazi, O. A., Amin, M. A., & Khaled, K. F. (2008). On the corrosion inhibition of low carbon steel in concentrated sulphuric acid solutions. Part I: Chemical and electrochemical studies. Corrosion Science, 50(8), 2258–2271. https://doi.org/10.1016/j.corsci.2008.06.005

[26] Zhang, W., Li, X., Zuo, X., Tan, B., Xu, C., & Zhang, S. (2021). Investigating the inhibitive effect of Davidia involucrata leaf extract as a biological eco-friendly inhibitor for copper in acidic medium. Journal of Molecular Liquids, 325, 115214. https://doi.org/10.1016/j.molliq.2020.115214

[27] Pareek, S., et al. (2018). A new insight into corrosion inhibition mechanism of copper in aerated 3.5% NaCl solution by eco-friendly imidazopyrimidine dye: Experimental and theoretical approach. Chemical Engineering Journal. https://doi.org/10.1016/j.cej.2018.08.079

[28] Gao, L., Peng, S., Huang, X., & Gong, Z. (2020). A combined experimental and theoretical study of papain as a biological eco-friendly inhibitor for copper corrosion in H_2SO_4 medium. Applied Surface Science, 511, 145446. https://doi.org/10.1016/j.apsusc.2020.145446

[29] Sanni, O., Popoola, A. P. I., & Fayomi, O. S. I. (2019). Temperature effect, activation energies and adsorption studies of waste material as stainless steel corrosion inhibitor in 0.5 M sulphuric acid. Journal of Bio-Tribo-Corrosion, 5(4), 0–8. https://doi.org/10.1007/s40735-019-0280-2

[30] Fayomi, O. S. I., Akande, I. G., & Popoola, A. P. I. (2018). Corrosion protection effect of chitosan on the performance characteristics of A6063 alloy. Journal of Bio- and Tribo-Corrosion, 4, 1–6. https://doi.org/10.1007/s40735-018-0192-6

[31] Agboola, O., et al. (2019). Adsorptive performance mechanism of the DNA of calf thymus gland (CTG DNA) on 3CR12 stainless steel as corrosion inhibitor in acidic medium. Journal of Bio- and Tribo-Corrosion, 5, 1–17. https://doi.org/10.1007/s40735-019-0245-5

[32] Sanni, O., Popoola, A. P. I., & Fayomi, O. S. I. (2021). Adsorption ability and corrosion inhibition mechanism of agricultural waste on stainless steel in chloride-contaminated environment. Materials Today: Proceedings, 43, 2215–2221. https://doi.org/10.1016/j.matpr.2020.12.349

[33] Dada, A. O., Olalekan, A. P., Olatunya, A. M., & Dada, O. (2012). Langmuir, Freundlich, Temkin and Dubinin–Radushkevich isotherm studies of equilibrium sorption of Zn^{2+} onto phosphoric-acid-modified rice husk. IOSR Journal of Applied Chemistry, 3(1), 38–45. https://doi.org/10.9790/5736-0313845

[34] Quraishi, M. A., Singh, A., Singh, V. K., Yadav, D. K., & Singh, A. K. (2010). Green approach to corrosion inhibition of mild steel in hydrochloric and sulphuric acid solutions by Murraya koenigii leaf extract. Materials Chemistry and Physics, 122(1), 114–122. https://doi.org/10.1016/j.matchemphys.2010.02.066

[35] Singh, A. K., & Quraishi, M. A. (2011). Investigation of the effect of disulfiram on corrosion of mild steel in hydrochloric acid solution. Corrosion Science, 53(4), 1288–1297. https://doi.org/10.1016/j.corsci.2011.01.002

[36] Ahamad, I., Prasad, R., & Quraishi, M. A. (2010). Adsorption and inhibitive properties of new Mannich bases of isatin derivatives on corrosion of mild steel in acidic media. Corrosion Science, 52(4), 1472–1481. https://doi.org/10.1016/j.corsci.2010.01.015

[37] Sanni, O., Popoola, A. P. I., & Fayomi, O. S. I. (2019). Temperature effect, activation energies and adsorption studies of waste material as stainless steel corrosion inhibitor in 0.5 M sulphuric acid. Journal of Bio-Tribo-Corrosion, 5, 1–8. https://doi.org/10.1007/s40735-019-0280-2

[38] Fayomi, O. S. I., Atiba, J. O., & Dauda, K. T. (2024). Electrochemistry and inhibitory evaluation of Musa paradisiaca particulates on AA6063 alloy for improved service life. Hybrid Advances, 6, 100234. https://doi.org/10.1016/j.hybadv.2024.100234

[39] Goh, K.-H., Lim, T.-T., & Chui, P.-C. (2008). Evaluation of the effect of dosage, pH and contact time on high-dose phosphate inhibition for copper corrosion control using response surface methodology (RSM). Corrosion Science, 50(4), 918–927. https://doi.org/10.1016/j.corsci.2007.12.008